

NASA Technical Memorandum 100143

Experimental Evaluation of Corner Turning Vanes—Summary

Royce D. Moore, Donald R. Boldman, Rickey J. Shyne,
and Thomas F. Gelder
*Lewis Research Center
Cleveland, Ohio*

Prepared for the
1987 Aerospace Technology Conference and Exposition
sponsored by the Society of Automotive Engineers
Long Beach, California, October 5-8, 1987



(NASA-TM-100143) EXPERIMENTAL EVALUATION OF
CORNER TURNING VANES Summary Report (NASA)
27 p Avail: NTIS EC A03/MF A01 CSCL 14B

N87-28571

Unclas
G3/09 0098897

EXPERIMENTAL EVALUATION OF CORNER TURNING VANES - SUMMARY

Royce D. Moore, Donald R. Boldman,
Rickey J. Shyne, and Thomas F. Gelder
National Aeronautics and Space Administration
Lewis Research Center
Cleveland, Ohio 44135

SUMMARY

Two types of turning vane airfoils (a controlled-diffusion shape and a circular-arc shape) have been evaluated in the high-speed and fan-drive corners of a 0.1-scale model of NASA Lewis Research Center's proposed Altitude Wind Tunnel. The high-speed corner was evaluated with and without a simulated engine exhaust removal scoop. The fan-drive corner was evaluated with and without the high-speed corner. Flow surveys of pressure and flow angle were taken for both the corners and the vanes to determine their respective losses. The two-dimensional vane losses were low; however, the overall corner losses were higher because three-dimensional flow was generated by the complex geometry resulting from intersection of the turning vanes with the end wall. The three-dimensional effects were especially pronounced in the outer region of the circular corner.

NOMENCLATURE

- P_S static pressure, N/cm^2
 P_T total pressure, N/cm^2
 q velocity head, $0.7 P_{S,M}$, N/cm^2
 ω_c corner loss coefficient, $(P_{T,in,c} - P_{T,out,c}) / q_{in,c}$
 ω_v vane loss coefficient, $(P_{T,in,v} - P_{T,out,v}) / q_{in,v}$

Subscripts:

- c corner
in inlet
out outlet
v vane
1 corner 1
2 corner 2

INTRODUCTION

The NASA Lewis Research Center's Altitude Wind Tunnel (AWT) first became operational in 1944 and was used for aeropropulsion research until 1958. The AWT was then converted to altitude chambers and was used for space research in the late 1950's and early 1960's. Since that time the tunnel has been inactive. In the early 1980's it was proposed that NASA Lewis rehabilitate the AWT for the aeropropulsion needs of the future. The proposed tunnel would accommodate tests involving fuel-burning engines, adverse weather conditions (including icing), and acoustics. As originally configured, the AWT had a maximum Mach number of 0.6 at 30 000 ft with a temperature capability of -69 °F. The proposed capabilities of the new tunnel (fig. 1) were Mach 0.92, 50 000 ft, and -40 °F, respectively.

When the tunnel was converted to altitude test chambers, all the internal components were removed. Since the proposed tunnel requirements were different from the original requirements, new components using the latest technology were required to meet the new objectives. In addition to a new high-speed leg (including settling chamber, contraction section, test section, and diffuser) and a new heat exchanger, four new sets of turning vanes and a new two-stage fan-drive system with variable inlet guide vanes (VIGV) were proposed (fig. 1). In corner 1 downstream of the test section (highest Mach number corner), an engine exhaust removal scoop would extend through the center of the turning vanes. The fan-drive shaft fairing would extend through the corner 2 turning vanes. Corners 3 and 4 would be clean (i.e., no centerbody would pass through the vanes). The proposed tunnel features and the new tunnel components have been described in detail by the authors (refs. 1 and 2).

Because of the magnitude of the proposed AWT rehabilitation a 0.1-scale modeling program was undertaken to ensure the technical soundness of the new component designs (refs. 3 to 7). The rehabilitation of the full-scale tunnel was not approved, but several of the scaled components were evaluated. Corners 1 and 2, the test section, and the contraction section were extensively tested (refs. 8 to 14).

This paper summarizes the significant results of the corner turning vane investigations. In each corner a controlled-diffusion airfoil design and a circular-arc airfoil design were evaluated. Both corners were tested over a range of Mach numbers. Corner 1 was tested with and without a simulated engine exhaust removal scoop. Corner 2 was investigated with and without corner 1 to determine interaction effects. The combined configuration (corner 1 and corner 2) was also tested with screen-generated distortion upstream of corner 1.

TURNING VANE DESIGN

One of the proposed changes for the existing tunnel was to increase the maximum test-section Mach number from near 0.6 to 0.92, with the new design value at 0.8. Since the tunnel shell existed, this requirement increased the Mach number at corner 1 to about 0.35. It was then proposed that an engine exhaust removal scoop be extended through the center of the corner 1 turning vanes (fig. 1). Therefore the corner 1 turning vanes would have to operate with Mach numbers greater than 0.40. Since there was a crossleg diffuser, the

corner 2 inlet Mach number was reduced to approximately 0.26. Corners 3 and 4 had inlet Mach numbers less than 0.10. The preliminary engineering report recommended a controlled-diffusion vane for corners 1 and 2 because a similar vane shape demonstrated good performance in an Ames wind tunnel (ref. 15). Since the Mach numbers were low for corners 3 and 4, the more conventional circular-arc vanes were recommended for those corners.

For the corner modeling program it was decided to test the more conventional circular-arc airfoil vane shapes as well as the recommended controlled-diffusion airfoil vanes. In both corners 1 and 2 a flat length of 10.67 cm (which formed an angle of 45° with both the upstream and downstream corners) was used as the vane holder (typical corner setup shown in fig. 2). Each set of vanes was mounted in the flat-length vane holder. For corner 1 the major axis of the elliptical corner was 116.38 cm, and the minor axis was 82.296 cm. The corresponding values for corner 2 were 133.99 and 94.743 cm. The two vane profiles are presented in Figure 3.

Vane A

The controlled-diffusion airfoil (vane A) was designed by an inverse method developed by Sanz (ref. 16). The inverse design code has an advantage in that the surface velocity distribution can be directly input. This allows control of the velocity diffusion and eliminates boundary layer separation. This calculation method accounts for the boundary layer displacement thickness and adjusts the vane shape to provide the manufacturing coordinates as output. For corner 1 there were 20 equally spaced vanes with a solidity of 1.89. For corner 2 there were 23 equally spaced vanes with a solidity of 1.92. The vane coordinate for corner 1 (ref. 8) differed slightly from those for corner 2 (ref. 9) because of the different inlet Mach numbers (0.35 versus 0.26). For the full-scale tunnel the same vane coordinates were proposed for both corners 1 and 2.

For corner 1 several changes in vane spacing and vane setting angle were investigated (ref. 8); however, in this paper only the original design (vane A) and the best configuration (vane A10 - all vanes reset -5° from design) are discussed. For corner 2 three modifications were made to the vane A configuration. One change was to reset all vanes -5° from design (vane A2). Next the outer vane was removed from the corner, and the corner was tested with the vanes at design angle (vane A3) and reset -5° (vane A4).

Vane B

The circular-arc airfoil (vane B) was designed by McFarland, who solved for the velocity distribution by using his blade-to-blade panel method code (ref. 17). The vane coordinates for corners 1 and 2 were identical (refs. 8 and 9). These vanes were designed for a solidity of 2.290, and this resulted in 24 vanes for corner 1 and 28 vanes for corner 2.

APPARATUS AND PROCEDURE

Test Apparatus

Because it was desired to be able to quickly change vanes, vane spacings, vane angles, and corners, several unique design features were included in the test apparatus. A choked nozzle assembly for flow measurement and a bellmouth inlet with a flow straightener were common for all configurations (fig. 4). For each corner a vane holder was made in sections. All vanes were made the same height and each vane was mounted in a separate holder (fig. 5). Spacers were used between each holder. Foam rubber was used to form the elliptical contour of the corners. These features allowed individual vane spacing and angle changes without disassembling.

Modular construction was used for the spool pieces, the instrumentation, and the rings (fig. 4). The spool pieces were made of a metal frame and a clear plastic wall. The instrumentation ring had four ports for total pressure rakes, boundary layer rakes, or traversing actuator probes located 90° apart. The ring could be physically rotated to survey other circumferential locations. The ring could also be positioned at different axial locations.

Corner 1 was tested clean to determine the best vane set to be installed with the simulated scoop (fig. 6). The wooden scoop was made in two parts with cutouts for the vanes. One part was mounted on each side of the turning vanes. For this configuration an instrumentation ring was mounted 1 diameter from the vanes, both upstream and downstream. Details of the corner 1 configurations are given in an earlier report (ref. 8).

The corner 2 configuration consisted of the crossleg diffuser, the fan-drive shaft fairing, the corner, and the fan VIGV's (fig. 7). This corner differed from corner 1 in that the shaft fairing crossed the inlet, whereas the scoop in corner 1 was aligned with the flow. Foam rubber was also used in corner 2 for the shaft fairing across the turning vanes. The IGV front portion was stationary and the rear portion was remotely variable. Details of the corner 2 configurations are given by Boldman et al. (ref. 9).

For the combined corner 1 and corner 2 configuration (fig. 8), the bellmouth and spool pieces ahead of the diffuser were removed, and corner 1 with the simulated scoop and vane A10 was installed. The bellmouth and spool pieces were then installed upstream of corner 1. To determine the effects of screen-generated distortions on the performance, another spool piece and distortion ring were added just downstream of the bellmouth and the flow straightener (fig. 9).

The modular design chosen offered great flexibility in conducting the experimental program. Both vane spacing and vane setting angle were investigated. It was also easy to change the vane set from vane A to B. Even changing from one corner to another or adding a corner could be accomplished rather quickly.

Instrumentation

The overall performance was determined from diametrical rakes. A typical rake is shown in figure 10(a). The rakes had 16 total pressure elements and

six total temperature elements. In addition to the diametrical rake four 8-element boundary layer rakes were used. A typical boundary rake is shown in figure 10(b). Each IGV had five total pressure elements mounted on the leading edge and four 8-element radial rakes downstream (fig. 10(c)). Static pressure taps were installed on the end walls, centerbodies, and vane surfaces. Details of the instrumentation and locations are given in earlier reports (refs. 8 to 11).

To determine vane losses, detailed surveys of the flow conditions were made with traverse probes. Surveys were made across two adjacent vane gaps in the outer, middle, and inner corner regions. The actuators mounted on top of the corner are shown in figure 11(a). To determine the total pressure and flow angle profiles downstream of the IGV, radial, and circumferential actuators (fig. 11(b)) were used. The locations of both the vane survey and IGV survey instrumentation were described previously (ref. 11).

RESULTS AND DISCUSSION

Corner 1 Performance Without Scoop

It was expected that corner performance would be better with vane A than with vane B. The results, however, yielded some surprises. As previously discussed (refs. 8 and 11), the vane performance as well as the corner performance was evaluated. Vane performance is summarized in figures 12 to 14. In the middle region of the corner, where the flow should be representative of two-dimensional flow, two vane passages were surveyed from the outer wall to the major axis. The two-dimensional vane loss coefficient of 0.05 and the vane surface Mach number distribution agreed quite well with design for vane A (fig. 12). The flow angles in the two-dimensional region showed overturning of approximately 3.5° over the design value of 45° . For vane B (fig. 13) the two-dimensional vane loss coefficient of 0.08 also agreed quite well with its design. However, the vane surface Mach number distribution indicated slight separation near the vane trailing edge. The two-dimensional flow angles for vane B showed about 2° of overturning.

The radial distribution of the vane loss coefficient (fig. 14) shows that for both vanes the three-dimensional effects of the end wall strongly influenced the loss coefficients near the end wall. Since the two-dimensional vane losses were less for vane A than for vane B, it was surprising when the corner loss coefficient for vane A was significantly greater than that for vane B (fig. 15). Visual observation of flow tufts indicated areas of flow separation in the outer corner region for vane A. An examination of the data indicated that high losses were occurring in the outer corner region. Vane A formed adverse geometry conditions with the end wall in the outer corner region. This adverse geometry probably contributed to the flow separation and to the higher corner losses in this circular corner.

If it had not been for the design versatility of the corner, which allowed for quick changes in angle and spacing, we would have concluded that vane B was a better turning vane design to be used in circular corners. However, several changes in vane setting angle and spacing were made (ref. 6) with vane A in an attempt to suppress the separated flow in the outer corner region. Similar changes in setting angle and spacing were not made with

vane B because the tufts and the data did not indicate flow separation in the outer corner region. Resetting all of the turning vanes -5° (vane A10) significantly reduced the corner losses (fig. 15). The vane loss coefficient did not change with the reset. The vane surface Mach number distribution did show the change in incidence angle. The turning vane performance in corner 1 without the scoop is summarized for the design Mach number of 0.35 in the following table:

	Vane A	Vane A10	Vane B
Vane (two-dimensional): Loss coefficient, ω_v	0.05	0.05	0.08
Exit flow angle, deg	48.5	43.5	47.0
Corner loss coefficient, ω_c	0.18	0.12	0.15

For the vane configurations investigated vane A10 gave the lowest corner losses and was selected to be used with the simulated engine exhaust removal scoop.

Corner 1 Performance With Simulated Scoop

The loss coefficient for corner 1 with the simulated scoop increased in part because the scoop was located in the low-loss two-dimensional region of the corner. Not only was more of the flow forced to the higher loss outer-wall region, but the intersection of the vanes with the scoop also produced another source for three-dimensional losses. The vane losses for vane A10 with and without the scoop are compared in figure 16. The two-dimensional vane loss coefficient increased from 0.05 to 0.08 with the scoop. These higher losses are attributed in part to the higher Mach number with the scoop (0.41 versus 0.35 without the scoop). The corner 1 losses with the scoop were based on measurements 1 diameter downstream of the corner (ref. 8). These losses were the same as the corner-plus-diffuser loss previously obtained (ref. 10) and repeated in figure 17. Also presented in figure 17 is the measured diffuser loss coefficient. Subtracting the diffuser losses from the corner-1-plus-diffuser losses resulted in the corner 1 losses with the scoop presented in the figure.

With the scoop the corner inlet Mach number increased to about 0.41; the estimated corner 1 loss coefficient at that condition was 0.14. The corresponding values without the scoop were 0.35 and 0.12.

Corner 2 Performance Without Corner 1

The results of the corner 2 vane evaluations were similar to those for corner 1. As previously discussed (refs. 9 and 11), the vane performance as well as the corner performance was evaluated. The vane performance is summarized in figures 18 to 20 for the middle region of the corner. Two vane passages were surveyed from the end wall to the centerbody. Both the end wall and the centerbody produced the same type of results. The two-dimensional region appeared to be from about 17 to 38 cm. The regions near the end wall and the centerbody tended to separate, with the vane wakes extending about one vane gap. This indicated a strong interaction of the end walls with the vanes

(three-dimensional effects). For both vane A3 (design setting with the first outer vane removed) and vane B, the vane surface Mach number distributions agreed quite well with their design distributions. These vane surface Mach number distributions were measured in the center passage and about halfway between the outer wall and the centerbody. However, the Mach number distribution for vane B indicated slight separation near the trailing edge. The vane flow angles seemed to vary more for corner 2 than for corner 1. For vane A3 the flow angle in the free-stream regions varied from about 47.5° to 50.0° . For vane B the flow angles were much closer to the design value of 45° .

As with the vane designs of corner 1, with corner 2 vane A (A3 at the design setting with the outer vane removed, and A4 reset -5° with the outer vane removed) had a lower two-dimensional loss coefficient than vane B (fig. 20). The effects of the centerbody and the end wall on the vane loss coefficient are quite evident in the figure. The vane loss coefficients in the two-dimensional region were 0.06 and 0.08 for vanes A and B, respectively.

The corner loss coefficients (fig. 21) for vanes A (design) and A3 (design setting with the outer vane removed) were essentially the same and were higher than those for vanes A2 and A4 (A and A3, respectively, reset -5°). The corner loss coefficient for vane B was about the same as those for vanes A2 and A4. Here again if it had not been for the versatility of the test rig, vane B would have been judged to be a lower loss design for the circular tunnel.

The results from both corners indicate that a very low-loss two-dimensional airfoil can be designed. However, in the real flow around corners the two-dimensional losses were not the predominate losses. The high losses appeared to be associated with the interaction of the turning vanes with the end walls (three-dimensional effects). For both corners the vane A two-dimensional losses were less than those for vane B. When the total effects were considered, there was essentially no difference in the overall corner losses in corner 2 for the two vanes.

Corner 2 Performance With Corner 1

Corner 2 performance was reevaluated with corner 1 added upstream. Corner 1 had the simulated engine exhaust removal scoop and vane A10. Vane performance is summarized in figures 22 and 23 for the middle region of corner 2. Again two vane passages were surveyed from the end wall to the centerbody. The two-dimensional region appeared to be from about 17 to 32 cm, as compared with 17 to 38 cm without corner 1. The flow angle in the free-stream region for vane A4 (reset -5° with the outer vane removed) agreed with the design value of 45° . The surface Mach number distribution reflected the 5° change in incidence angle due to the reset. The vane B surface Mach number distribution indicated slight separation over the vane trailing edge.

When the vane loss coefficient was originally calculated for the corner 2 vanes with corner 1 upstream, the values were higher than those without corner 1. For all individual corner data the average inlet velocity head was used in the vane loss calculation because the entering flow was assumed to be uniform. However, when corner 1 was added upstream of corner 2, the flow entering corner 2 was no longer uniform. With corner 1 and vane B in corner 2 the flow migrated away from the end wall and the centerbody and toward the middle region

(fig. 24). By assuming that the local inlet velocity head is proportional to the average inlet velocity head by the square of the velocity ratio with and without corner 1, the vane loss coefficient was calculated. These values (fig. 25) were only slightly different from those obtained without corner 1.

The corner 2 loss coefficient (fig. 26) was significantly less with corner 1 than without it. As indicated in figure 24, the flow had shifted from the high loss end-wall regions to the lower loss two-dimensional region. The lower corner loss coefficient was attributed to lower loss in the outer wall region of corner 2, which in turn resulted from the lower momentum inflow to this region caused by the higher three-dimensional losses in the outer wall region of corner 1.

Effects of Distortion on Corner Performance

For the data presented thus far in the paper the inlet flow into the corners was uniform. From a preliminary examination of the limited available data for the high-speed leg configuration, a pressure profile was obtained upstream of corner 1. The pressure profile was based on fixed instrumentation just upstream of corner 1 without the scoop. In an attempt to simulate the pressure profile two radial distortion screens were tested. A circumferential distortion screen that was intended to simulate the engine exhaust removal scoop at its maximum expected angle of attack was also tested. These three screen configurations are discussed in detail by Gelder, et al. (ref. 10).

The measured inlet pressure contours for the three screen configurations (fig. 27) showed that the radial distortion obtained with the screens was less than that measured in the high-speed leg. The effects of the screen-generated distortion on the corner loss coefficient are presented in figure 28. Although there was more scatter in the data than with uniform flow, there was no consistent difference between uniform or distorted flows or between vane sets in corner 2.

CONCLUDING REMARKS

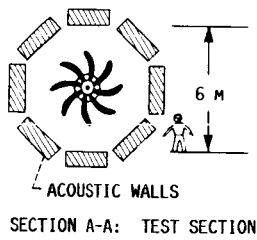
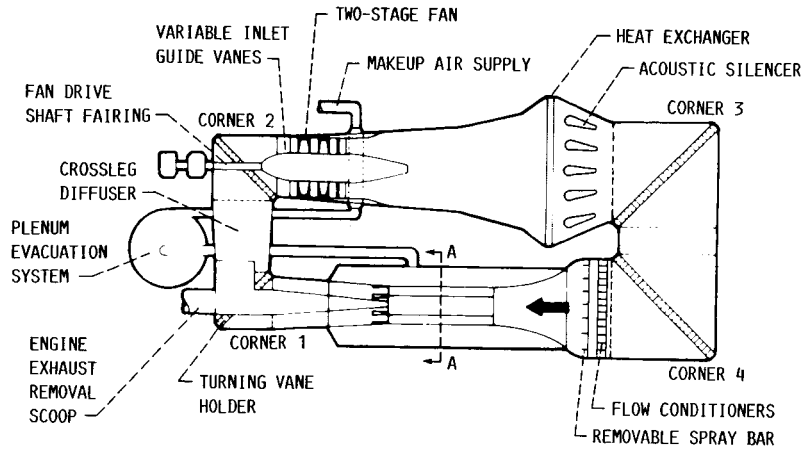
The results of this investigation show that high Mach number turning vanes can be designed with very low losses. The two-dimensional vane loss coefficient was 0.05 for a controlled-diffusion shape (vane A) and 0.08 for a circular-arc shape (vane B). The corner loss coefficient was significantly higher for these circular corners. We attributed this to the high three-dimensional losses associated with the end walls. The controlled-diffusion vane, in particular, formed a very adverse geometry where it met the outer wall. These adverse geometry conditions increased the losses in the outer corner such that the overall corner losses were greater for vane A than for vane B. Resetting vane A -5° (vane A10) did relieve part of the problem and produced a lower corner loss coefficient than for vane B. In rectangular corners the adverse geometry between vane and tunnel wall will not exist. Therefore the corner loss coefficient should be much closer to the vane loss coefficient. And the controlled-diffusion vane with its lower vane loss coefficient would have a lower overall corner loss than the circular-arc shape (vane B).

The results from this investigation also indicate that upstream corners may have beneficial effects. Corner 2 loss coefficients were lower when it was tested downstream of corner 1 than when it was tested alone. This was due to lower losses in the outer wall region of corner 2, which in turn resulted from the lower momentum inflow to this region caused by the high three-dimensional losses in the outer wall region of corner 1.

REFERENCES

1. R. Chamberlin, "The Altitude Wind Tunnel (AWT) - A Unique Facility for Propulsion System and Adverse Weather Testing." AIAA Paper 85-0314, Jan. 1985. (NASA TM-86921.)
2. B. Blaha and R.J. Shaw, "The NASA Altitude Wind Tunnel: Its Role in Advanced Icing Research and Development." AIAA Paper 85-0090, Jan. 1985. (NASA TM-86920.)
3. J.M. Abbott, J.H. Diedrich, J.F. Groeneweg, L.A. Povinelli, L. Reid, J.J. Reinmann, and J.R. Szuch, "Analytical and Physical Modeling Program for the NASA Lewis Research Center's Altitude Wind Tunnel (AWT)." AIAA Paper 85-0379, Jan. 1985. (NASA TM-86919.)
4. C.E. Towne, L.A. Povinelli, W.G. Kunik, K.K. Muramoto, C.E. Hughes, and R. Levy, "Analytical Modeling of Circuit Aerodynamics in the New NASA Lewis Altitude Wind Tunnel." AIAA Paper 85-0380, Jan. 1985. (NASA TM-86912.)
5. T.F. Gelder, R.D. Moore, J.M. Sanz, and E.R. McFarland, "Wind Tunnel Turning Vanes of Modern Design." AIAA Paper 86-0044, Jan. 1986. (NASA TM-87146.)
6. C.C. Ciepluch, R.R. Burley, D.E. Groesbeck, J.C. Marek, and R.D. Moore, "Progress in the Lewis Research Center Altitude Wind Tunnel (AWT) Modeling Program." AIAA Paper 86-0757, Mar. 1986. (NASA TM-87194.)
7. R.J. Shyne, R.D. Moore, and D.R. Boldman, "Comparison of Analytical and Experimental Performance of a Wind-Tunnel Diffuser Section." NASA TM-88795, 1986.
8. R.D. Moore, D.R. Boldman, and R.J. Shyne, "Experimental Evaluation of Two Turning Vane Designs for High-Speed Corner of 0.1-Scale Model of NASA Lewis Research Center's Proposed Altitude Wind Tunnel." NASA TP-2570, 1986.
9. D.R. Boldman, R.D. Moore, and R.J. Shyne, "Experimental Evaluation of Two Turning Vane Designs for Fan-Drive Corner of 0.1-Scale Model of NASA Lewis Research Center's Proposed Altitude Wind Tunnel." NASA TP-2646, 1987.
10. T.F. Gelder, R.D. Moore, R.J. Shyne, and D.R. Boldman, "Experimental Evaluation of Turning Vane Designs for High-Speed and Coupled Fan-Drive Corners of 0.1-Scale Model of NASA Lewis Research Center's Proposed Altitude Wind Tunnel." NASA TP-2681, 1987.

11. R.D. Moore, R.J. Shyne, D.R. Boldman, and T.F. Gelder, "Detailed Flow Surveys of Turning Vanes Designed for 0.1-Scale Model of NASA Lewis Research Center's Proposed Altitude Wind Tunnel." NASA TP-2680, 1987.
12. D.E. Harrington, R.R. Burley, and R.R. Corban, "Experimental Evaluation of Wall Mach-Number Distributions of Octagonal Test Section Proposed for NASA Lewis Research Center's Altitude Wind Tunnel (AWT)." NASA TP-2666, 1986.
13. R.R. Burley, and D.E. Harrington, "Experimental Evaluation of Honeycomb/Screen Configurations and Short Contraction Section for NASA Lewis Research Center's Proposed Altitude Wind Tunnel." NASA TP-2692, 1987.
14. R.R. Burley and D.E. Harrington, "Experimental Evaluation of Blockage Ratio and Plenum Evacuation System Flow Effects on Pressure Distribution for Bodies of Revolution in 0.1-Scale Model Test Section of NASA Lewis Research Center's Proposed Altitude Wind Tunnel." NASA TP-2702, 1987.
15. J.M. Sanz, E.R. McFarland, N.L. Sanger, T.F. Gelder, and R.H. Cavicchi, "Design and Performance of a Fixed, Nonaccelerating Guide Vane Cascade That Operates Over an Inlet Flow Angle Range of 60 Degrees." Journal of Engineering for Gas Turbines and Power, Vol. 107, No. 2, Apr. 1985, pp. 477-484.
16. J.M. Sanz, "Improved Design of Subcritical and Supercritical Cascades Using Complex Characteristics and Boundary Layer Correction." (NASA Contract NAS3-22531.) NASA CR-168166, 1983.
17. E.R. McFarland, "A Rapid Blade-to-Blade Solution for Use in Turbomachinery Design." Journal of Engineering for Gas Turbines and Power, Vol. 106, No. 2, Apr. 1984, pp. 376-382.



MACH NUMBER	0 TO 0.9+
ALTITUDE, M	0 TO 17 000+
TOTAL TEMPERATURE, °C	-40 TO 15
TEST-SECTION ACOUSTIC LEVEL, dB (OASPL)	120

FIGURE 1. - CAPABILITIES OF MODIFIED AND REHABILITATED AWT.

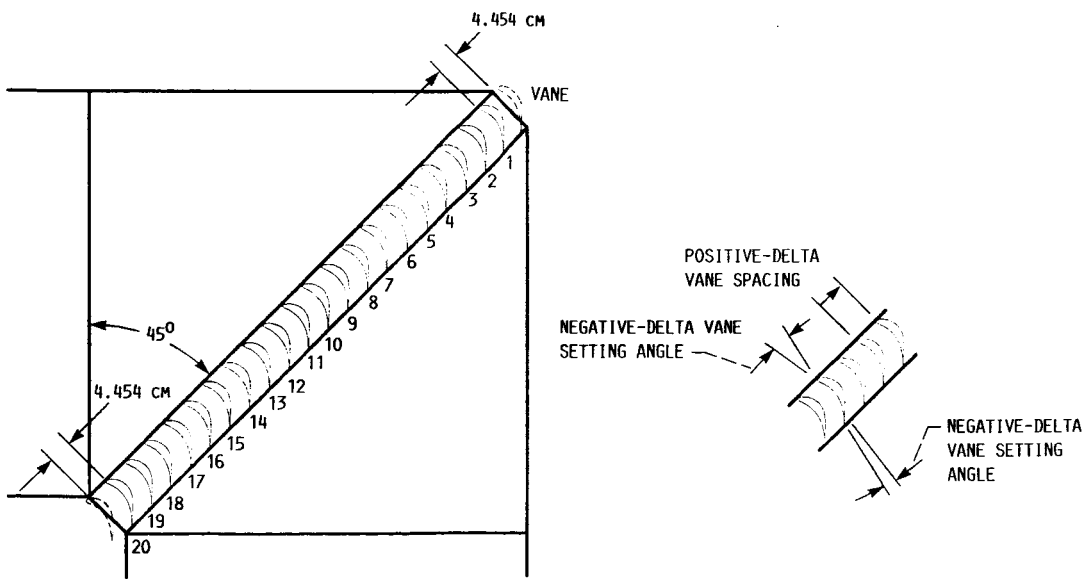
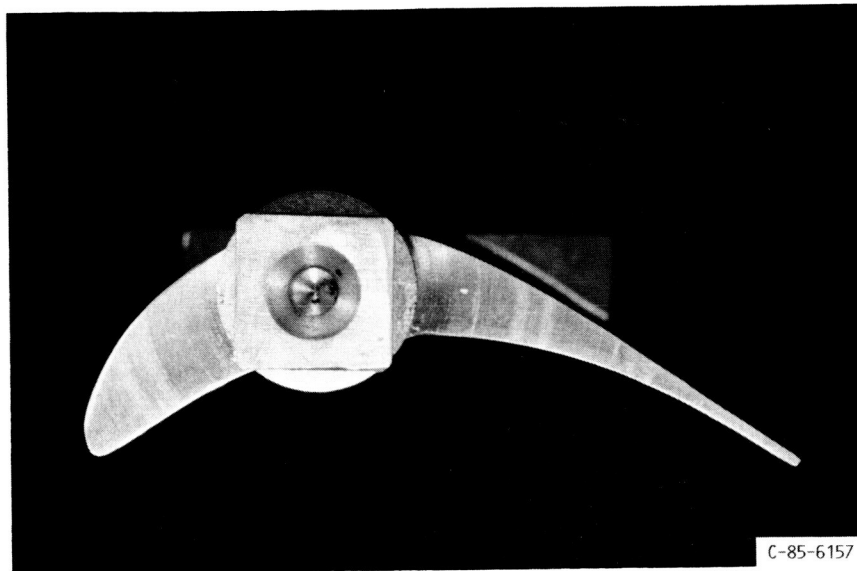


FIGURE 2. - SCHEMATIC SHOWING VANE A SETUP (20 VANES) IN CORNER 1 (ALONG MAJOR AXIS).

ORIGINAL PAGE IS
OF POOR QUALITY



(A) VANE A (CONTROLLED DIFFUSION).



(B) VANE B (CIRCULAR ARC).

FIGURE 3. - CORNER 2 TURNING VANES.

ORIGINAL PAGE IS
OF POOR QUALITY

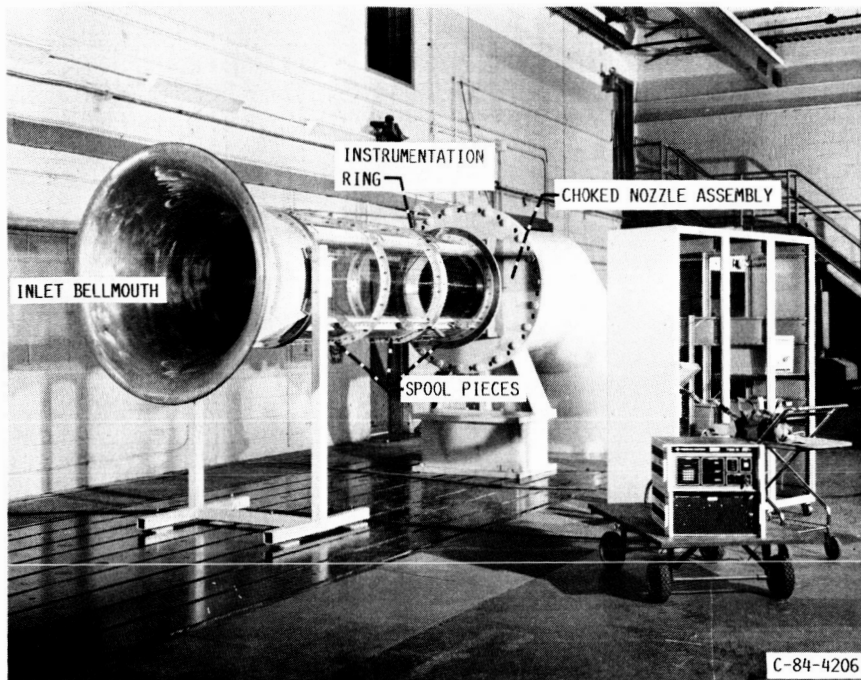


FIGURE 4. - INLET BELLMOUTH AND CHOKED NOZZLE ASSEMBLIES FOR SCALED MODELS.

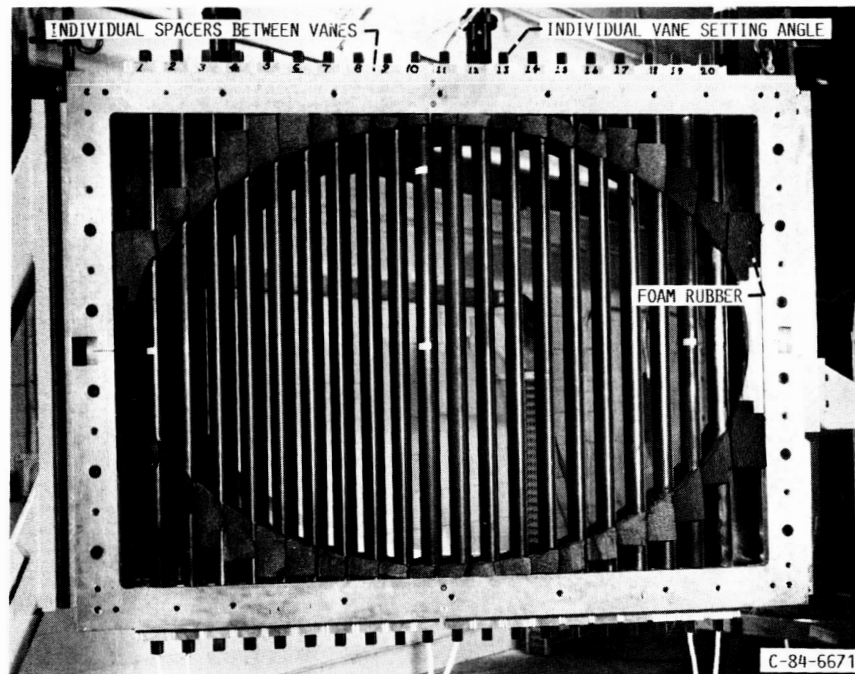
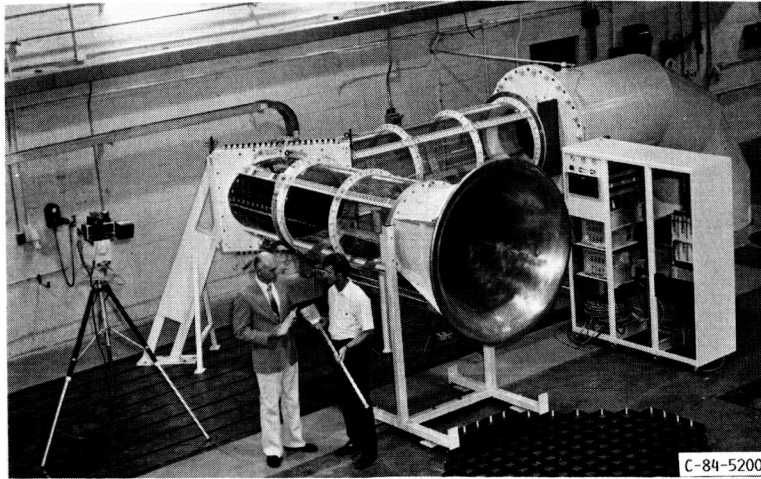
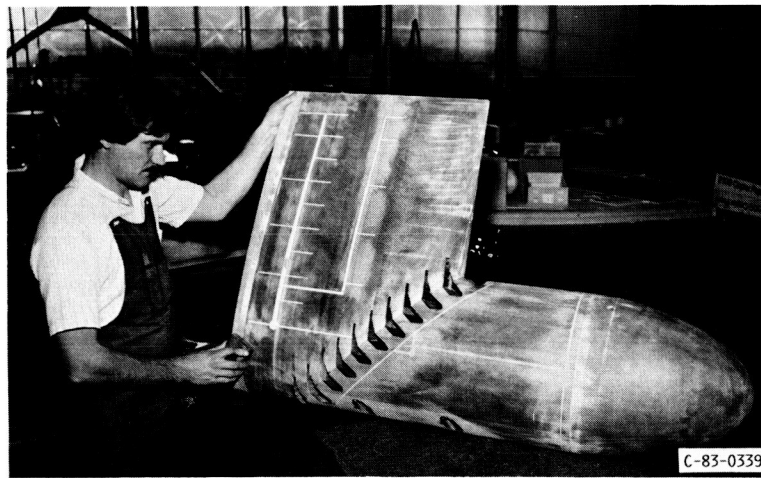


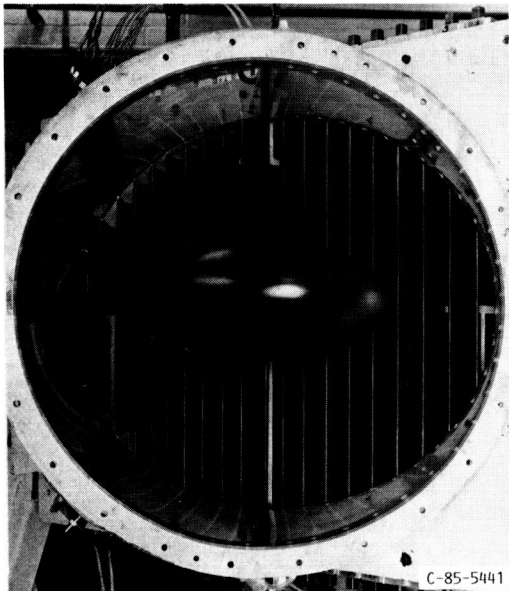
FIGURE 5. - CORNER 1 VANE HOLDER.



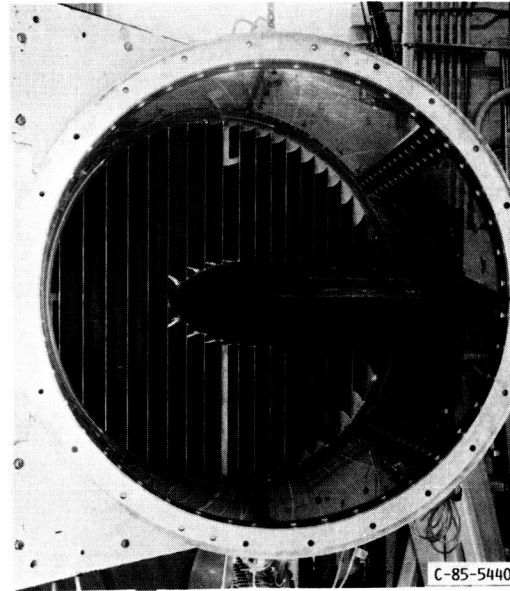
(A) CORNER 1.



(B) SIMULATED ENGINE EXHAUST SCOOP.



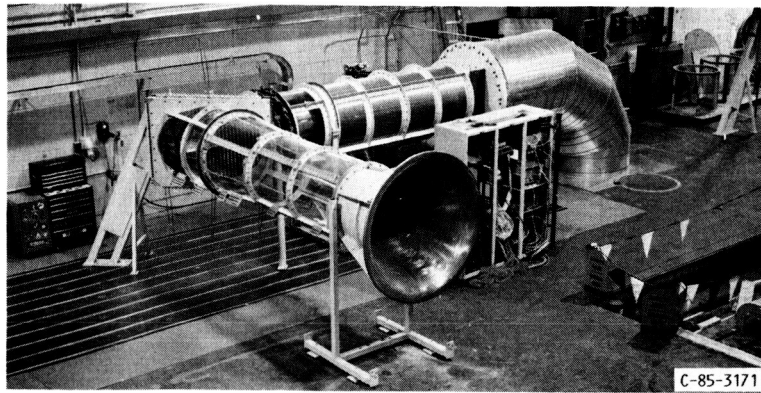
(C) CORNER INLET WITH SCOOP.



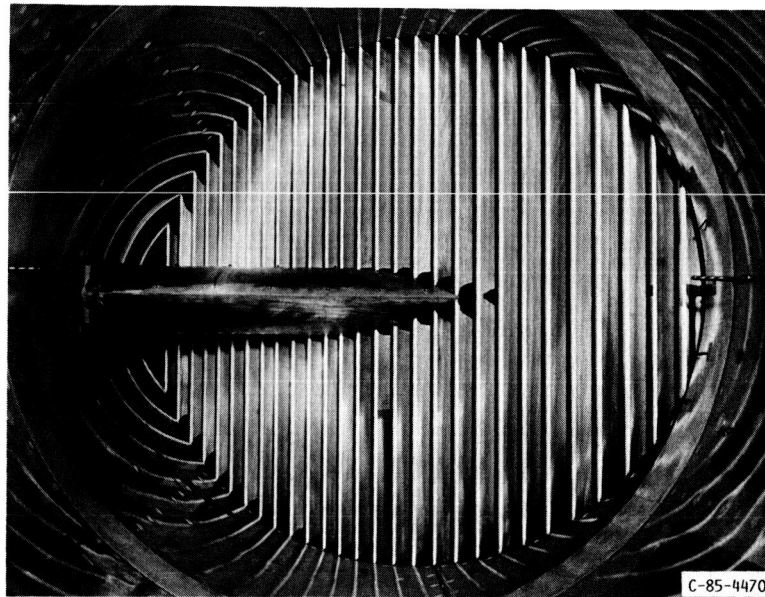
(D) CORNER OUTLET WITH SCOOP.

FIGURE 6. - CORNER 1 WITH SIMULATED ENGINE EXHAUST SCOOP.

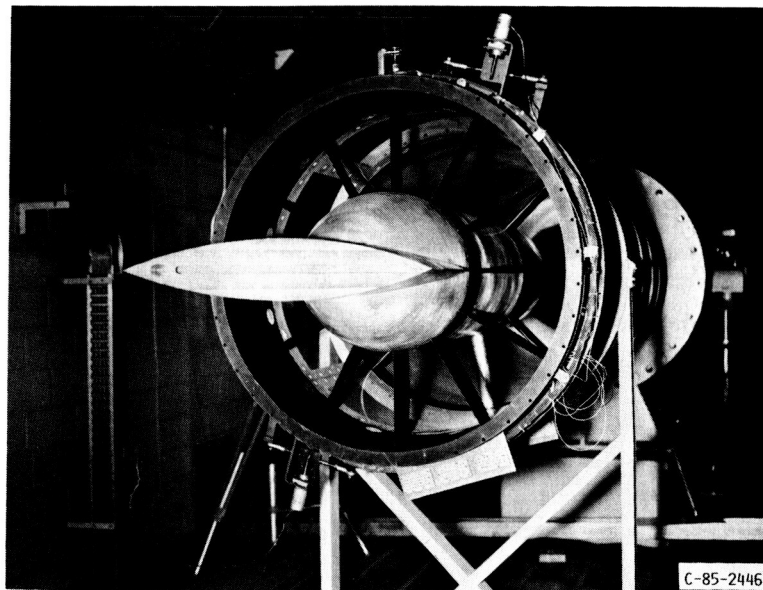
ORIGINAL PAGE IS
OF POOR QUALITY



(A) CORNER 2.

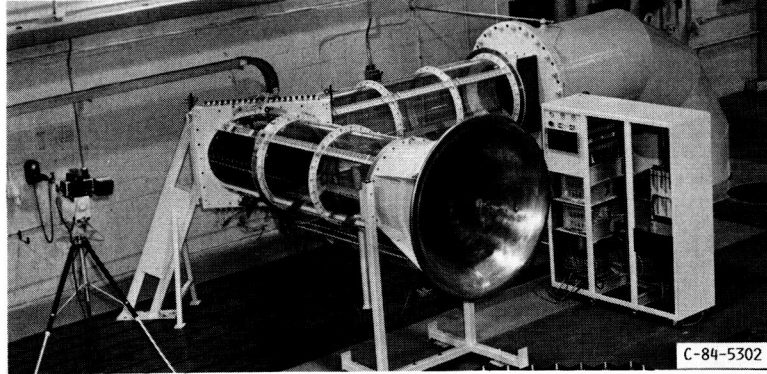


(B) CORNER INLET WITH SHAFT FAIRING.

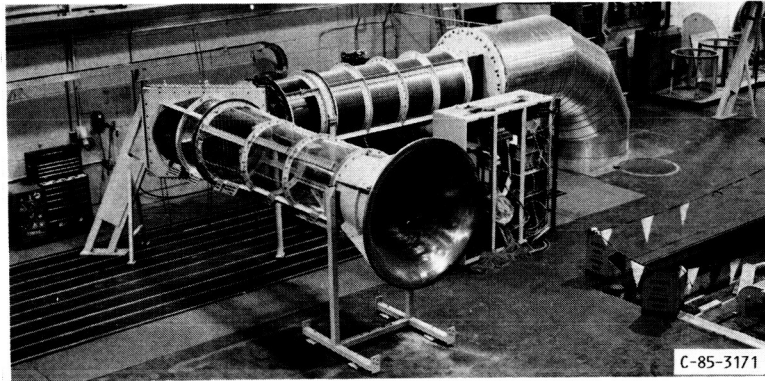


(C) DOWNSTREAM SHAFT FAIRING WITH FAN INLET GUIDE VANES.

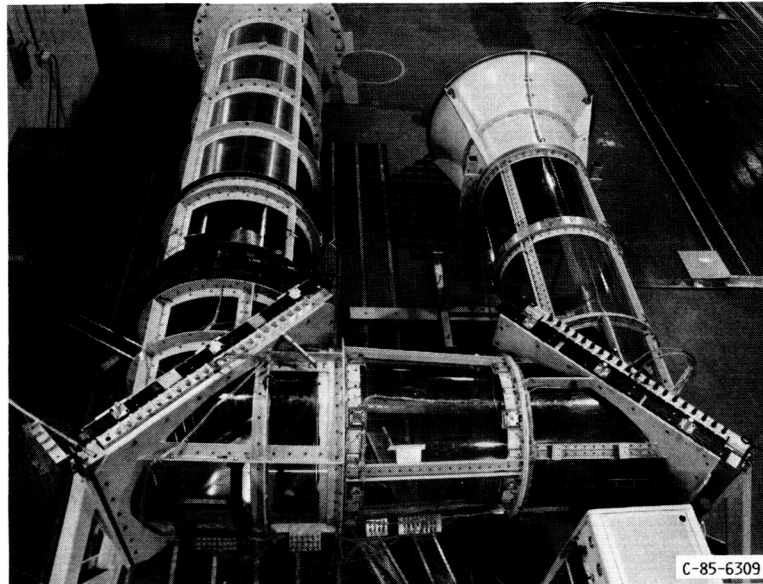
FIGURE 7. - CORNER 2 WITH FAN DRIVE SHAFT FAIRING.



(A) CORNER 1.



(B) CORNER 2.



(C) CORNERS 1 AND 2.

FIGURE 8. - CORNERS 1 AND 2 TEST CONFIGURATIONS.

ORIGINAL PAGE IS
OF POOR QUALITY

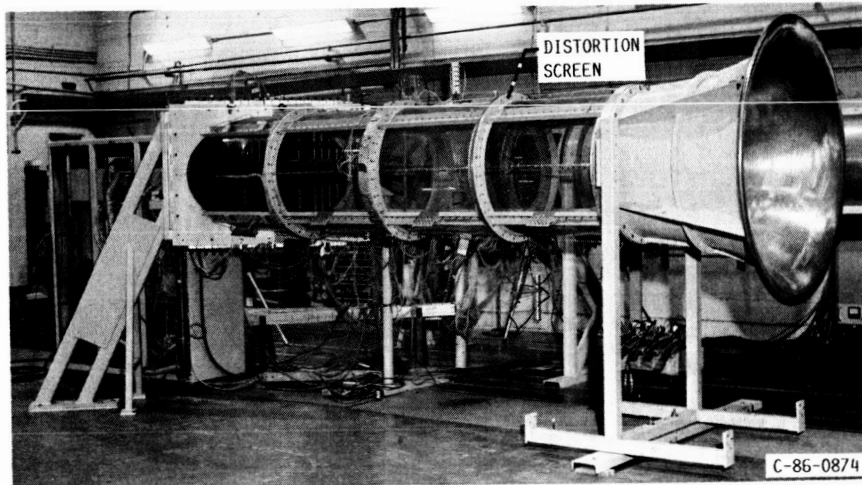
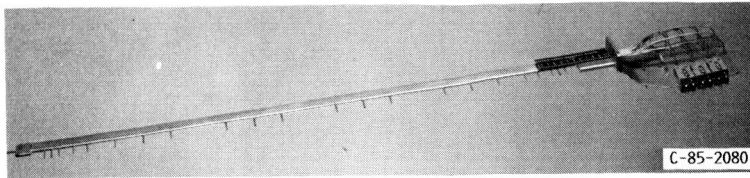
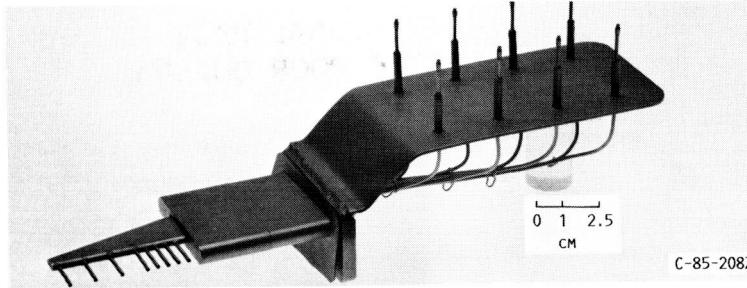


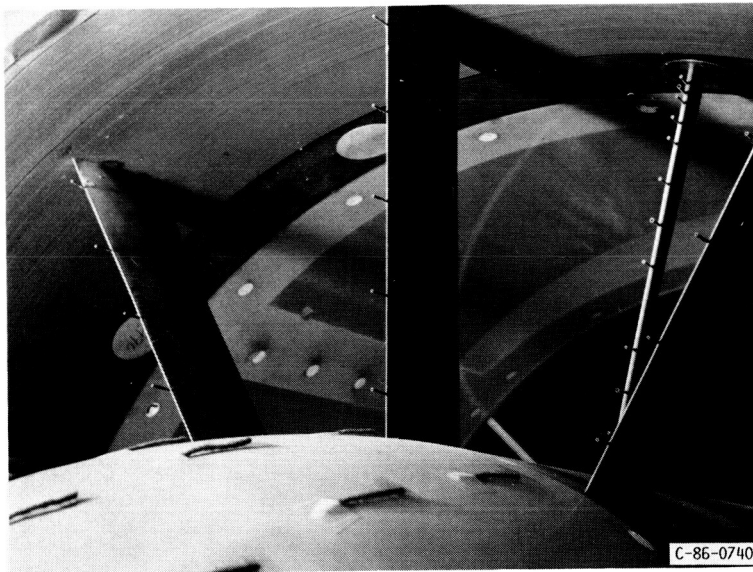
FIGURE 9. - CORNERS 1 AND 2 WITH UPSTREAM DISTORTION SCREEN.



(A) DIAMETRICAL RAKE.



(B) BOUNDARY LAYER RAKE.



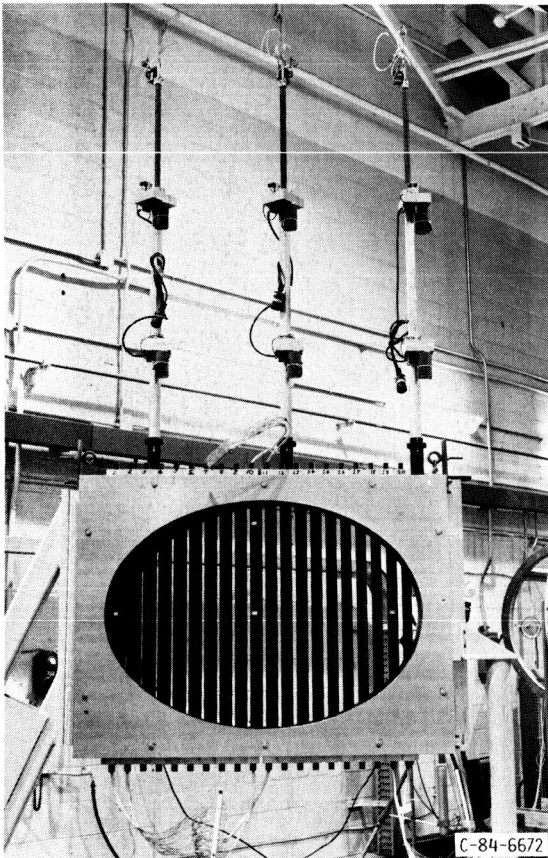
(C) IGV LEADING EDGE AND DOWNSTREAM RAKE.



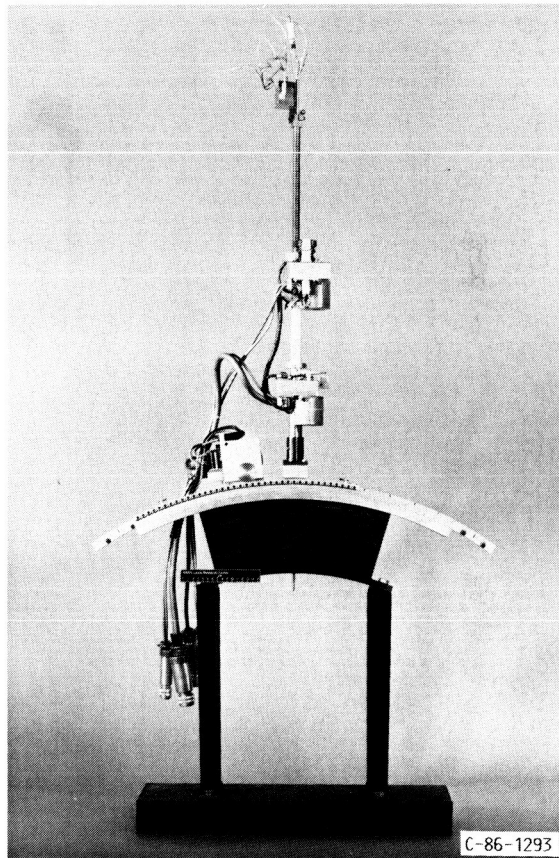
(D) TRAVERSE PROBE.

FIGURE 10. - INSTRUMENTATION.

ORIGINAL PAGE IS
OF POOR QUALITY



(A) VANE EXIT SURVEY.



(B) IGV EXIT SURVEY.

FIGURE 11. - ACTUATORS.

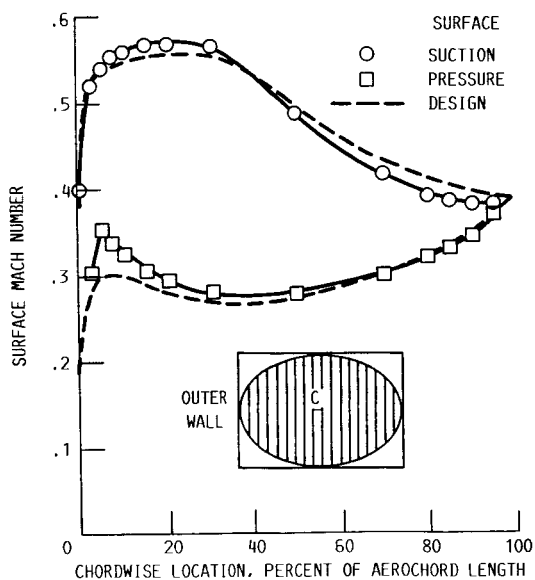
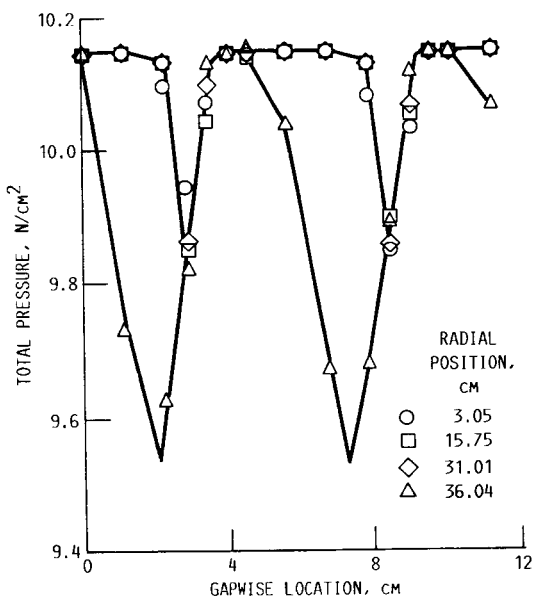
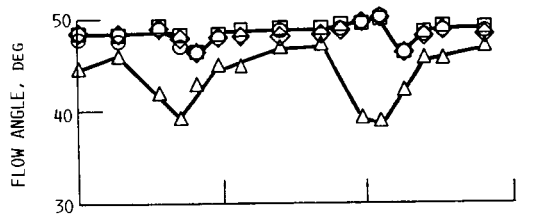


FIGURE 12. - VANE A PERFORMANCE IN CORNER 1 WITHOUT SCOOP. TWO-DIMENSIONAL FLOW REGION; NOMINAL INLET MACH NUMBER, 0.35.

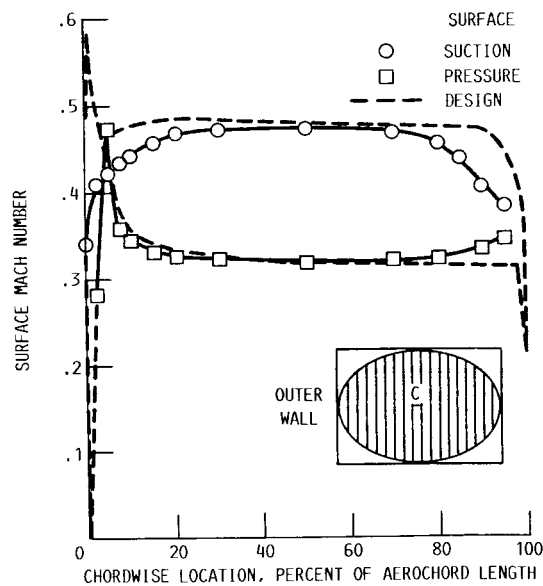
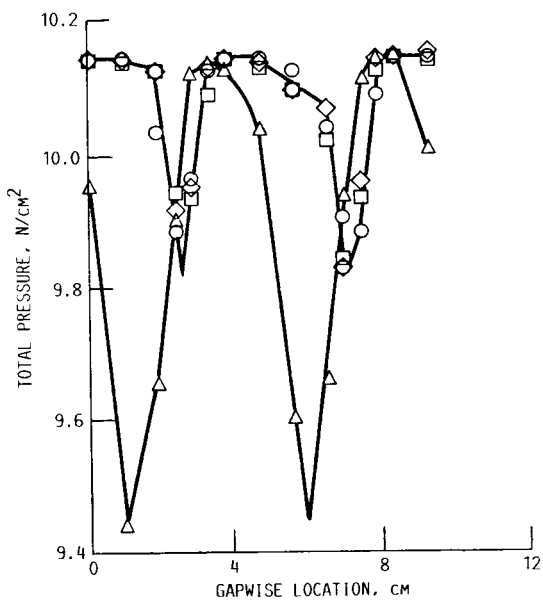
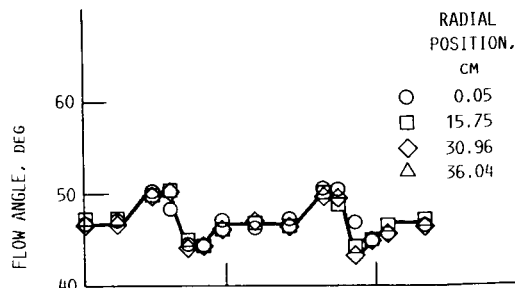


FIGURE 13. - VANE B PERFORMANCE IN CORNER 1 WITHOUT SCOOP. TWO-DIMENSIONAL FLOW REGION; NOMINAL INLET MACH NUMBER, 0.35.

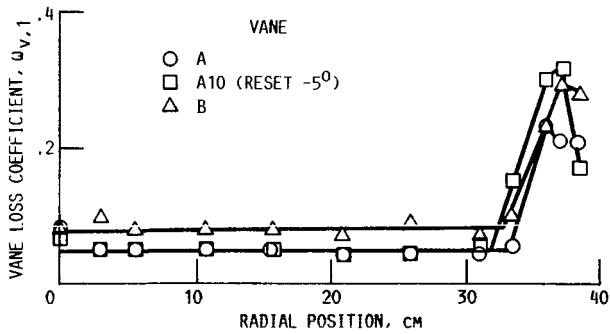


FIGURE 14. - VANE LOSS COEFFICIENT IN MIDDLE REGION OF CORNER 1. NOMINAL AIRFLOW, 73 KG/SEC; NOMINAL INLET MACH NUMBER, 0.35.

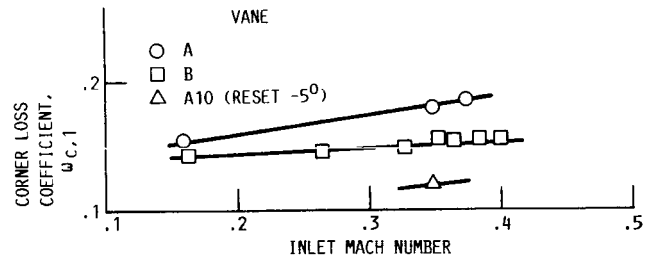


FIGURE 15. - LOSS COEFFICIENT AS FUNCTION OF INLET MACH NUMBER FOR CORNER 1 WITHOUT SCOOP.

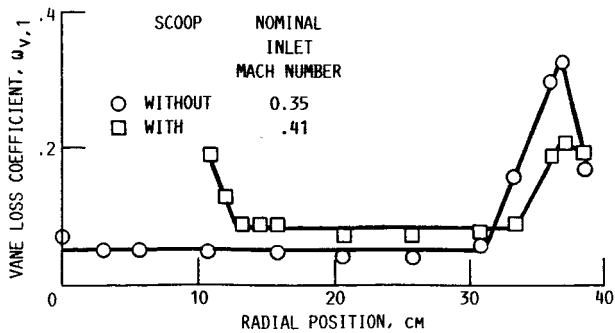


FIGURE 16. - EFFECT OF SIMULATED SCOOP ON VANE LOSS COEFFICIENT IN MIDDLE REGION OF CORNER 1 WITH VANE A10. NOMINAL AIRFLOW, 73 KG/SEC.

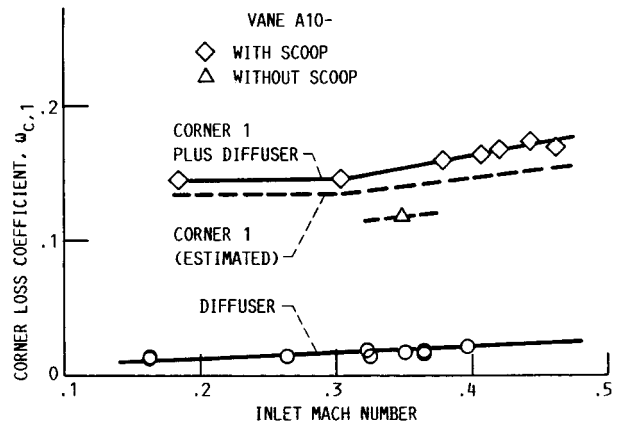


FIGURE 17. - EFFECT OF SIMULATED SCOOP ON CORNER 1 LOSS COEFFICIENT FOR VANE A10.

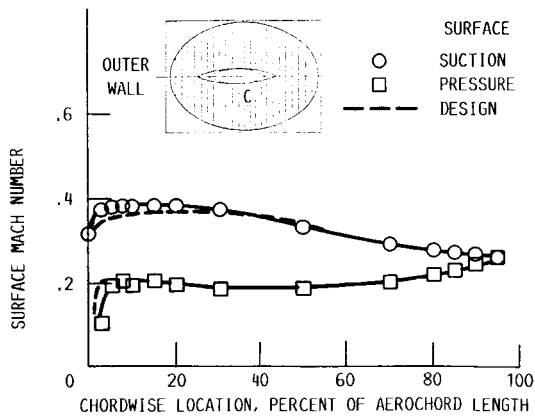
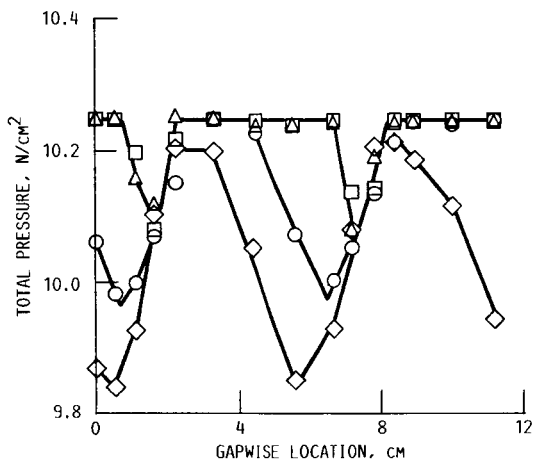
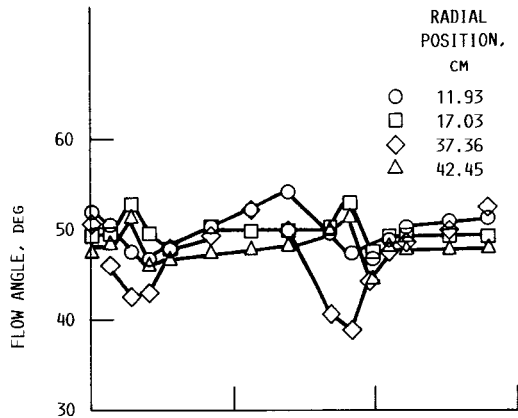


FIGURE 18. - VANE A3 PERFORMANCE IN CORNER 2 WITHOUT CORNER 1. TWO-DIMENSIONAL FLOW REGION; NOMINAL INLET MACH NUMBER, 0.24.

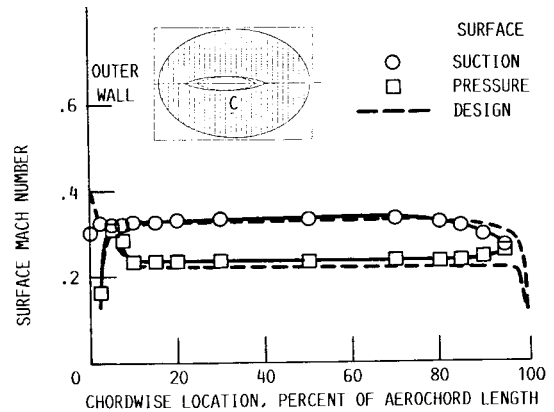
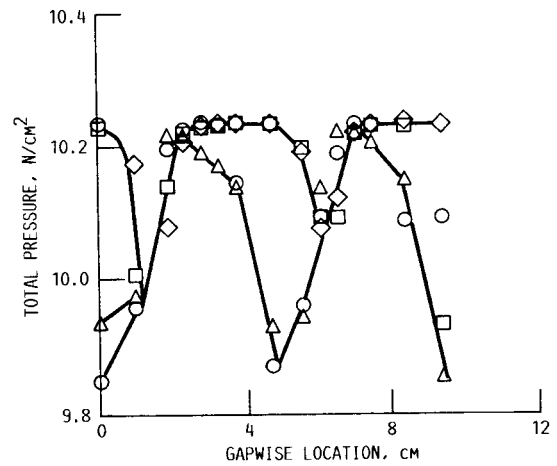
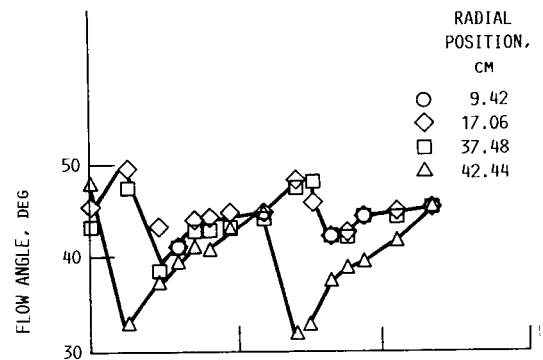


FIGURE 19. - VANE B PERFORMANCE IN CORNER 2 WITHOUT CORNER 1. TWO-DIMENSIONAL FLOW REGION; NOMINAL INLET MACH NUMBER, 0.24.

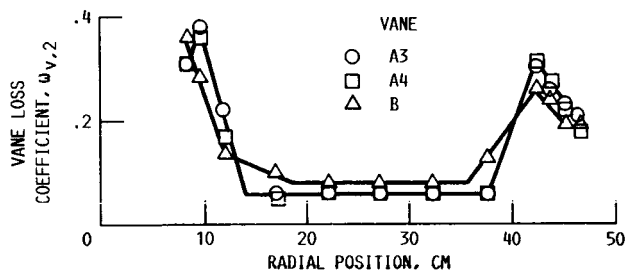


FIGURE 20. - VANE LOSS COEFFICIENT IN MIDDLE REGION OF CORNER 2 WITHOUT CORNER 1. NOMINAL AIRFLOW, 69 kg/sec; NOMINAL INLET MACH NUMBER, 0.24.

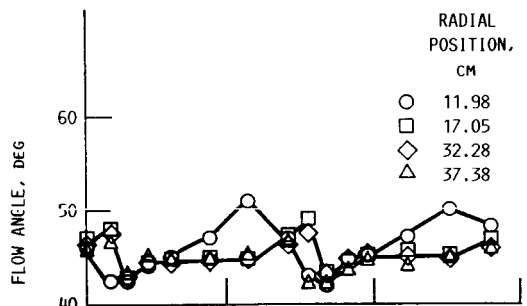


FIGURE 21. - CORNER 2 LOSS COEFFICIENT WITHOUT CORNER 1 AS FUNCTION OF INLET MACH NUMBER. DATA FAIRING BASED ON LEAST-SQUARES FIT

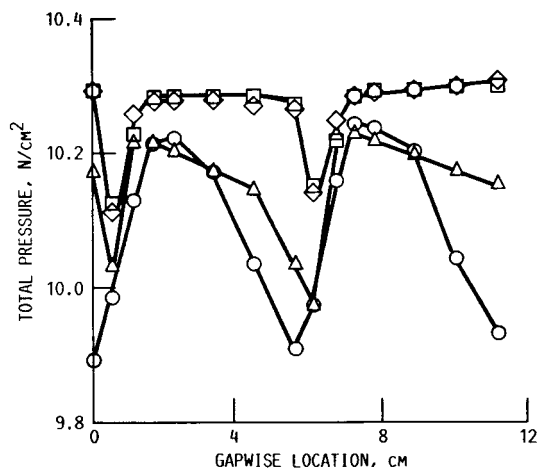
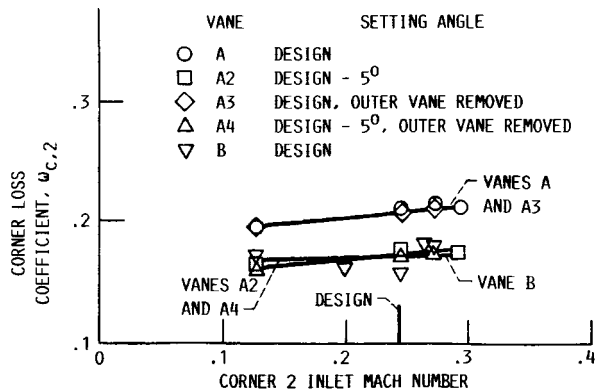


FIGURE 22. - VANE A4 PERFORMANCE IN CORNER 2 WITH CORNER 1. TWO-DIMENSIONAL FLOW REGION; NOMINAL INLET MACH NUMBER, 0.26.



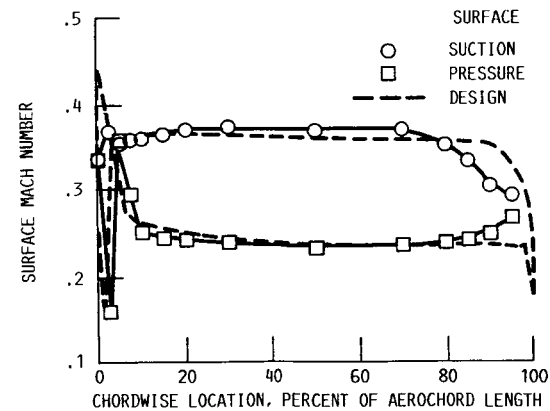
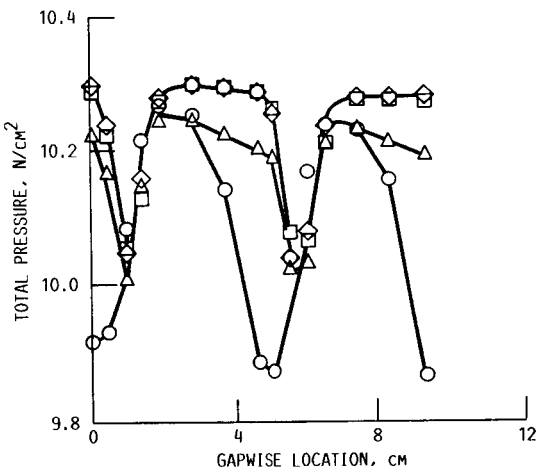
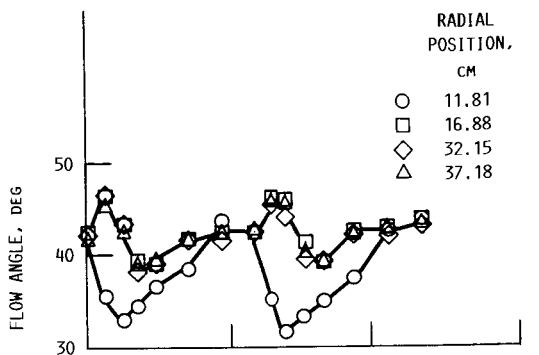


FIGURE 23. - VANE B PERFORMANCE IN CORNER 2 WITH CORNER 1. TWO-DIMENSIONAL FLOW REGION; NOMINAL INLET MACH NUMBER, 0.26.

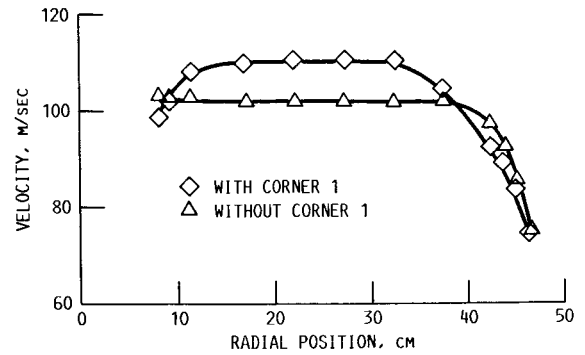


FIGURE 24. - EFFECT OF CORNER 1 ON RADIAL DISTRIBUTION OF VELOCITY DOWNSTREAM OF VANE B IN CORNER 2. MIDDLE REGION; NOMINAL AIRFLOW, 73 KG/SEC.

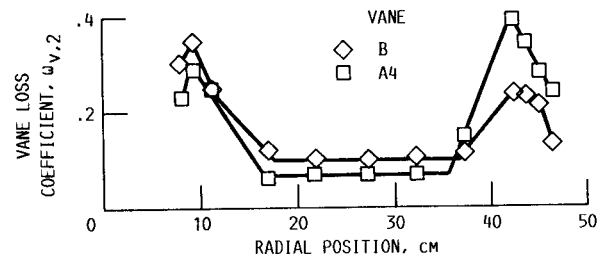


FIGURE 25. - CORNER 2 VANE LOSS COEFFICIENT UNDER LOCAL CONDITIONS. MIDDLE REGION; NOMINAL AIRFLOW, 73 KG/SEC; NOMINAL INLET MACH NUMBER, 0.26.

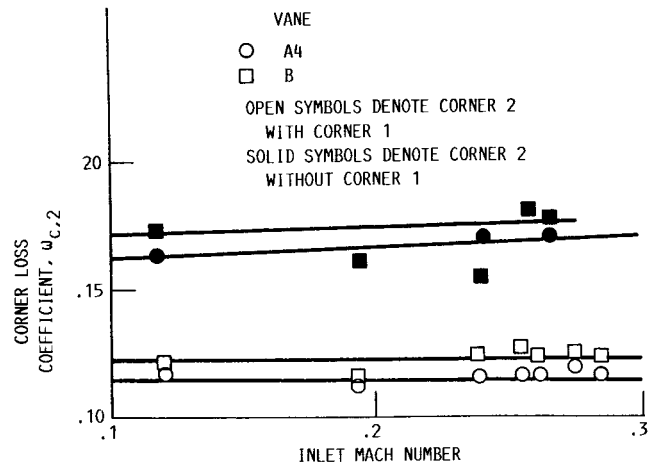
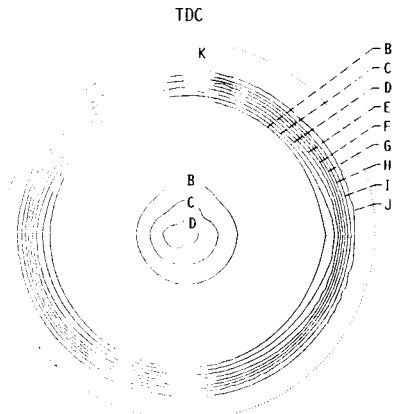
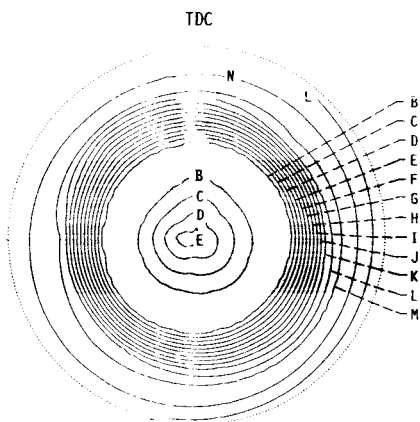


FIGURE 26. - EFFECT OF CORNER 1 ON CORNER 2 LOSS COEFFICIENT.

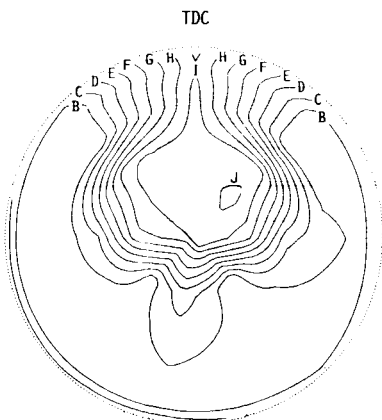


(a) 15-PERCENT TIP RADIAL SCREEN.

CONTOUR	INLET PRESSURE, N/cm ²
B	10.35
C	10.28
D	10.22
E	10.15
F	10.08
G	10.01
H	9.95
I	9.87
J	9.81
K	9.75
L	9.69
M	9.63
N	9.56

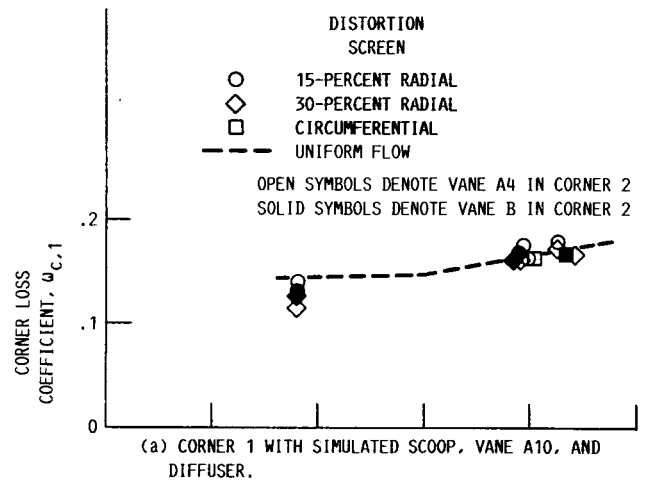


(b) 30-PERCENT TIP RADIAL SCREEN.

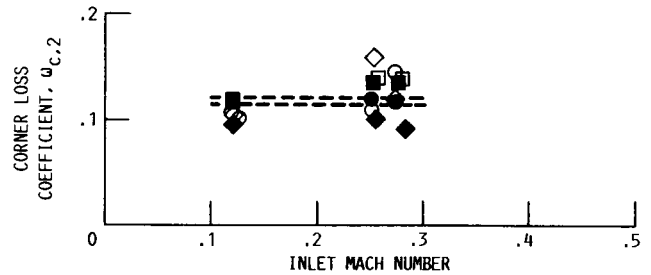


(c) CIRCUMFERENTIAL SCREEN.

FIGURE 27. - CORNER 1 INLET PRESSURE CONTOURS (LOOKING DOWNSTREAM) IMPOSED BY DISTORTION SCREENS. NOMINAL AIRFLOW, 72.8 KG/SEC; NOMINAL CORNER 1 INLET MACH NUMBER, 0.40.



(a) CORNER 1 WITH SIMULATED SCOOP, VANE A10, AND DIFFUSER.



(b) CORNER 2 WITH CORNER 1.

FIGURE 28. - EFFECT OF SCREEN-GENERATED DISTORTIONS ON CORNER LOSS COEFFICIENT.

1. Report No. NASA TM-100143		2. Government Accession No.		3. Recipient's Catalog No.	
4. Title and Subtitle Experimental Evaluation of Corner Turning Vanes - Summary				5. Report Date	
				6. Performing Organization Code 535-05-01	
7. Author(s) Royce D. Moore, Donald R. Boldman, Rickey J. Shyne, and Thomas F. Gelder				8. Performing Organization Report No. E-3695	
				10. Work Unit No.	
9. Performing Organization Name and Address National Aeronautics and Space Administration Lewis Research Center Cleveland, Ohio 44135				11. Contract or Grant No.	
				13. Type of Report and Period Covered Technical Memorandum	
12. Sponsoring Agency Name and Address National Aeronautics and Space Administration Washington, D.C. 20546				14. Sponsoring Agency Code	
15. Supplementary Notes Prepared for the 1987 Aerospace Technology Conference and Exposition, sponsored by the Society of Automotive Engineers, Long Beach, California, October 5-8, 1987.					
16. Abstract Two types of turning vane airfoils (a controlled-diffusion shape and a circular-arc shape) have been evaluated in the high-speed and fan-drive corners of a 0.1-scale model of NASA Lewis Research Center's proposed Altitude Wind Tunnel. The high-speed corner was evaluated with and without a simulated engine exhaust removal scoop. The fan-drive corner was evaluated with and without the high-speed corner. Flow surveys of pressure and flow angle were taken for both the corners and the vanes to determine their respective losses. The two-dimensional vane losses were low; however, the overall corner losses were higher because three-dimensional flow was generated by the complex geometry resulting from the turning vanes intersecting the end wall. The three-dimensional effects were especially pronounced in the outer region of the circular corner.					
17. Key Words (Suggested by Author(s)) Wind tunnel turning vanes Cascades Corner flows				18. Distribution Statement Unclassified - unlimited STAR Category 09	
19. Security Classif. (of this report) Unclassified		20. Security Classif. (of this page) Unclassified		21. No of pages 26	22. Price* A03